Advances in Materials
2024; 13(1): 1-9
http://www.sciencepublishinggroup.com/j/am
doi: 10.11648/j.am.20241301.11
ISSN: 2327-2503 (Print); ISSN: 2327-252X (Online)

Fundamental Investigation of the Adsorption of Antimicrobial Agents on Modified Calcium Carbonate and Silica and Its Potential Application in Food Packaging

Abdul Haseeb, Beko Mesic*, Jörgen Samuelsson

Department of Engineering and Chemical Sciences, Karlstad University, Karlstad, Sweden

Email address:

abdul.haseeb@kau.se (Abdul Haseeb), beko.mesic@kau.se (Beko Mesic), jorgen.samuelsson@kau.se (Jörgen Samuelsson)

*Corresponding author

To cite this article:

Abdul Haseeb, Beko Mesic, Jörgen Samuelsson. (2024). Fundamental Investigation of the Adsorption of Antimicrobial Agents on Modified Calcium Carbonate and Silica and Its Potential Application in Food Packaging. *Advances in Materials*, *13*(1), 1-9.
https://doi.org/10.11648/j.am.20241301.11

Received: November 27, 2023; **Accepted**: December 21, 2023; **Published**: January 8, 2024

Abstract: Antimicrobial packaging has emerged as one of the most effective packaging systems in prolonging shelf life and maintaining food quality. For an effective system, a controlled and gradual release of antimicrobial agents into food items over time is crucial. Modified Calcium Carbonate (MCC), known for its diverse applications in pharmaceuticals and drug delivery, could act as a potential carrier for such agents in packaging. In this context, a fundamental study of the adsorption of two reference antimicrobial agents, Benzoic Acid (BA) and Thymol (TM), was carried on MCC and silica in solvents of different polarities. Based on the initial adsorption study, the adsorption isotherms of the two compounds were acquired by batch method in different solvents and then the adsorption data was modeled using adsorption isotherm models. Here, we found that *n*-Heptane was the most efficient solvent for both BA and TM on both adsorbents. From the outcome of the adsorption study, a model dispersion coating was prepared by mixing MCC (loaded with BA) with latex binder. Then the effect of latex binder on the rate of BA release from MMC was investigated by conducting desorption study using simulated body fluid as the desorbent solution at 4°C, comparing MCC with and without latex. It was found that the release rate of BA from our latex model dispersion coating was 31 time slower than that of MMC without latex. This indicates the potential application of our model dispersion coating in antimicrobial packaging.

Keywords: Antimicrobial Packaging, Modified Calcium Carbonate, Silica, Benzoic Acid, Thymol, Adsorption, Desorption, Adsorbent

1. Introduction

Microbial contamination is one of the most common causes of food spoilage [1-3]. Although the traditional methods of food preservation like drying, freezing, heating, fermentation, refrigeration, adding antimicrobial (AM) agents modified atmosphere and irradiation have been in use for a long time, they have their limitations and their applications are conditional [2, 4-6]. Food packaging systems have been developed as an alternative tool to extend the shelf life and maintain quality of food. The key function of packaging is to act as a barrier between external environment and food, and prevent deterioration by the actions of microorganisms, moisture, gases, dust as well as mechanical forces [4, 7, 8].

In recent times, in addition to extended shelf life, food safety has become a major public concern not only due to food-borne pathogens but also due to outbreaks [4, 9]. Currently one of the focuses in food packages systems is to develop innovative approaches to prevent microbial activities in food to meet stringent safety requirements and extend shelf life [10-12]. In one of such approaches called antimicrobial packaging (AMP) which falls under the category of active packaging, the antimicrobial (AM) agent is added to the packaging system or the antimicrobial function is achieved by the use of polymer having antimicrobial property [5, 9, 10, 13]. These AMPs are more effective than introducing AM agents directly to food during processing or handling, for two reasons. First, the AM agents incorporated

to the packaging, enables slow and constant release of AM agents which function over longer period of time. Second, upon direct addition, the AM agents diffuse rapidly into the bulk of the food and the food constituents may deactivate the AM agents by neutralization, hydrolysis, dilution etc., thereby reducing the effectiveness of AM agents [4, 5].

Depending on the mode of antimicrobial action, the AM agents in the AMP may be present in the form of Sachets or pads inside the packing system which release the AM in the form of vapors in the head space above the packaged food [9, 14, 15]. Alternatively, the AM agents may be incorporated into the packaging system through simple blending or layered on the surface of the packaging or immobilized onto the packaging system. In case of immobilization, the AM agent only come in contact with the food on the surface and the AM agents do not migrate or diffuse into the food. In the remaining cases, the AM agents migrate or diffuse into the food content [4, 9, 14]. Incorporation of the AM agents into the packaging system can adversely affect the physical and mechanical properties of thermally processed materials such tensile strength, elongation, thermal stability, barrier properties to moisture and gases, among others, if they are not compatible with the polymers [4,14]. One approach would be to coat the packaging substrates with a carrier polymer containing antibacterial agents [16–18]. An alternative approach would be the use of environmentally friendly dispersion coatings incorporated with porous/mesoporous fillers loaded with AM. Most common porous/mesoporous fillers are silica gel (SiO_2) and Calcium Silicate (Ca_2SiO_4). They are effective adsorbents but are quite expensive. A good approach would be use of relatively cheap porous filler such as Modified calcium carbonate (MCC).

The MCCs are demonstrating a broad variety of new uses. They are being suggested as excipients, pharmaceutical ingredients and drug delivery agents. The porous nature of calcium carbonate provides excellent ingredient stability, delayed biodegradability, is readily manufactured, tasteless, stable, nontoxic and biocompatible [19–21]. MCC loaded with antimicrobial agent and then incorporated as coating into the packaging system would serve the dual purpose of preserving food through antimicrobial action and improving the properties of coating. Alternatively, if used as Sachets or pads, they would sever as excellent carriers of AM agents because they are biocompatible and safe. Röcker et al. have shown that MCC loaded with Linoleic acid (LA) and oleic acid (OA) sealed in tea bags inside the packaging work as effective oxygen scavengers [22]. Rüegg et al. have effectively used MCC incorporated as coating into the packaging materials and then loaded with thyme and rosemary essential oil as AM agents for the preservation of cooked meat [13]. Wang et al. showed that different antioxidant incorporated into gelatin-calcium carbonate films possess significant antioxidant activity [23]. However, a systematic study of the use MCC as potential carrier of AM agents in food packaging is lacking. In this respect, fundamental studies, such as the adsorption capacity of AM agents onto MCC, uptake and release rates, and the effect of solvents and other factors, need to be conducted.

The loading capacity of AM agents onto the MCC and its release and uptake rates would be studied through Adsorption isotherms. Adsorption isotherm describe the relationship between the amount of solute adsorbed on the surface and in liquid phase at equilibrium at a given temperature. Many different adsorption isotherm models have been used in literature to describe the adsorption process [24]. Benzoic Acid (BA) was chosen as model compound because BA is one of the most commonly used preservatives in food products, beverages and cosmetics, beside many other applications as *p*H regulator, flavoring agents, viscosity-controlling agent, solvent etc., in variety of products. It is a weak organic acid, safe in relatively higher concentration and effective against a wide range of bacteria, fungi and some viruses [25]. On the other hand, Thymol (TM) was selected as reference compound because TM is a naturally occurring neutral compound and has found widespread application as an antibacterial, antifungal, antioxidant, antimutagenic, wound healing, insecticide, medical disinfectant agent. The most common use of TM is as food preservative because of its antimicrobial and antioxidant activity and is safe at relatively higher concentration [26, 27].

The aim of this study is to gain better understanding of the adsorption process of some potential ant-microbial compounds onto MCC using silica as reference surface. As model compounds here we use BA and TM as adsorbates, and acetonitrile (MeCN), ethanol (EtOH), *n*-heptane (*n*-Hept) and aqueous phosphate buffer as solvents. The adsorption isotherms will be acquired using batch method and the adsorption data will be modeled using isotherm models. The potential of MCC as carrier of AM agents will also be investigated. The long-term goal is to use MCC particles with physically adsorbed anti-microbial compounds within food packaging application to prolong shelf life.

2. Theory

In this study the adsorption isotherms were determined using batch method. The adsorbed amount of solute, q_e, in a batch adsorption process could be estimated from the mass balance over the system.

$$mq_0 + VC_0 = mq_e + VC_e, \tag{1}$$

where m is the mass of the adsorbent, V is the volume of the liquid phase, q_e is the adsorbed amount (e.g., g solute per g adsorbent) at equilibrium, q_0 is the adsorbed amount at start (in our case q_0=0), C_e and C_0 is the concentration of the solute at equilibrium and at the start, respectively.

On can now rearrange Eq. (2) to find an expression of q_e:

$$q_e = q_0 + \frac{V}{m}(C_0 - C_e). \tag{2}$$

By determining the adsorbed amount at several different concentrations of solute in the liquid phase, an adsorption isotherm can be determined. One of the simplest adsorption isotherm models with limited saturation capacity is the

Langmuir model.

$$q_e = q_s \frac{KC_e}{1+KC_e}, \quad (3)$$

where q_s is the monolayer saturation capacity and K is the association equilibrium constant. A n-Langmuir model is simply a linear combination of n independent Langmuir adsorption isotherms. Bi-Langmuir represents two, tri-Langmuir three, and so on.

One problem with modeling the adsorption processes with adsorption isotherms is that several different adsorption isotherm models exist that can describe the determined data. The selection of adequate adsorption model is rather hard. Here we use a three-way approach: (1) plotting a Scatchard plot to determine the type of adsorption model (2) calculating the adsorption energy distribution (AED) to determine the heterogeneity of the adsorption process, and finally (3) fitting the raw adsorption data to different adsorption models that fulfill point (1) and (2) mentioned above.

A Scatchard plot is just another way of plotting the adsorption isotherm, q_e / C_e vs C_e. A linear Scatchard plot indicates that the adsorption process follows a Langmuir adsorption isotherm model. A concave Scatchard plot indicates a heterogeneous adsorption process. In such cases, models such as the Tóth model and bi-Langmuir are commonly used.

An AED is an extension of an adsorption isotherm to a continuous distribution of independent homogeneous sites across the range of adsorption energies under investigation, which can be written as:

$$q_e(C) = \int_{\ln K_{min}}^{\ln K_{max}} f(\ln K) \cdot \theta(C_e, \ln K)\, \mathrm{d} \ln K, \quad (4)$$

where f is the adsorption energy distribution, K the adsorption isotherm parameters, and θ (C_e, ln K) the kernel function, many different functions can be used and here we are using the Langmuir model. Langmuir kernel functions are a good choice for adsorption processes with convex adsorption isotherms that don't contain any inflection points. ln K represents the adsorption energy, as described by the Arrhenius equation. The integral is solved over the energy spaced ln K_{min} and ln K_{max} that is estimated by $0.1/C_{max}$ and $10/C_{min}$, respectively, where C_{min} and C_{max} are the lowest non zero concentration and the highest concentration used in the experimental adsorption isotherm. In this study the AED were numerically solved using the expectancy maximization method [28]. The AED is used to identify the type of heterogeneity described by the adsorption process. If the AED contains more than one distribution, this indicates that adsorption isotherm models with these properties, such as bi-Langmuir or tri-Langmuir, are required to properly model the data.

3. Materials and Methods

3.1. Materials and Instruments

Modified calcium carbonate (MCC) supplied by Omya International AG (Oftringen, Switzerland) and silica powder purchased from Supelco (Sweden) were used as adsorbents. The properties of the adsorbents are listed in Table 1. Benzoic Acid (BA) and Thymol (TM) of high purity grade (>98%) purchased from Sigma-Aldrich (Steinheim, Germany) were used as solutes. HPLC grade absolute EtOH, MeCN and *n*-Hept were supplied by Fisher scientific. Sodium di-hydrogen phosphate and disodium hydrogen phosphate were purchased from Sigma-Aldrich (Steinheim, Germany). Ultra-pure water with a resistivity of 18.2 MΩ·cm from Milli Q EQ7000 water purification system was used for preparation of buffer and Simulated Body Fluid (SBF). A UV-Vis spectrometer (UV-1800, Shimadzu) was used to measure the absorbance of solutions in different experiments. Analytical Balance (Mettler Toledo AE-160) was used to measure the weights of adsorbents and solutes and EBA-20 Hettich Zentrifugen was used for centrifugation of samples. HPZ 175 Experimental SB Latex (Styron Europe GmbH, Germany) was used as binder for preparation of model dispersion coatings. Solid content of the binder was 49.5%, the *p*H was 8.7 and viscosity was 56 mPa·s.

Table 1. *Properties of the adsorbents.*

	MCC	**Silica powder**
Appearance	Powder	Fine particles
Colour	White	White
*p*H stability	≥ 7.4	-
Particle size (µm)	6.6	40 - 63
Specific Surface Area (m^2g^{-1})	53	≥ 480
Density ($g{\cdot}mL^{-1}$)	0.13	0.7 - 0.85

3.2. Methods

3.2.1. Preparation of Standards and Stock Solutions

Stock solution of BA and TM (1 $g{\cdot}L^{-1}$ each) were prepared individually in *n*-Hept, EtOH, MeCN and aqueous phosphate buffer (pH: 7.5) for solvent screening and adsorption isotherms acquisition. The desired concentrations of BA and TM for the acquisition of adsorption isotherms were prepared by dilution of these stock solutions in relevant solvents. Separate stock solutions (1 $g{\cdot}L^{-1}$) of BA and TM were prepared individually in *n*-Hept, EtOH, MeCN and phosphate buffer in order to create calibration curve of these compounds in the relevant solvents. Similarly, a separate stock solution of BA (1 $g{\cdot}L^{-1}$) in Simulated Body Fluid (SBF) was prepared to create calibration curve of BA in SBF. Calibration standards of BA were prepared by dilution of this stock solution in SBF. The dissolution of BA in *n*-Hept and SBF requires sonication. SBP was prepared according to the procedure described by Kokubo at al. [29].

3.2.2. Solvent Screening for Adsorption Process

Four solvents, MeCN, EtOH, *n*-Hept and 20 mM phosphate aqueous buffer at *p*H 7.5 were selected to study the adsorption of the two model compounds BA and TM on both adsorbent MCC and Silica. The purpose was to select suitable solvent/solvents in which the given compounds would adsorb better to the surface of the adsorbents and then further use these solvents for the process of adsorption

isotherm acquisition and evaluation.

In order to measure the amount of BA adsorbed to the surface, a known amount of approximately 0.2 g of adsorbent (MCC, Silica) was weighed individually (Mettler Toledo Analytical Balance AE-160) into a 15 mL Falcon centrifuge tube. After that, 10 mL of 1·g·L^{-1} of BA solution in the respective solvent (*n*-Hept, EtOH, MeCN and aqueous buffer) was added to the falcon centrifuge tube using pipette. The tubes were then briefly and vigorously shaken by hand before being placed in a 25°C temperature-controlled water bath for 1 hour. The falcon tubes were removed from the water bath every 15 minutes and shaken briefly and vigorously for 1 minute. It was then centrifuged (EBA-20 Hettich Zentrifugen) for 15 minutes at 4000 rpm. After that, the supernatant was decanted and filtered through a 0.2 µm PTFE syringe filter before being collected in a clean and stoppered glass vial. The supernatants were then analyzed by UV-Vis spectrometer (UV-1800 Shimadzu). Four samples of BA were analyzed in each solvent for both adsorbents. Similarly, a blank sample experiment containing no BA in the solvent was carried for both adsorbents. Similar procedure was repeated for TM in each solvent for both adsorbents. Then the amount of BA and TM adsorbed to the surface were calculated using equation 2.

The wavelength for BA in EtOH and MeCN was found to be 272 nm, in *n*-Hept it was 247 nm and 224 nm in SBF. Similarly, the wavelength for TM in EtOH and MeCN were found to be 276 and 279 nm, and for *n*-Hept 267 nm. Calibration curves of BA and TM in each solvent were generated by preparation of calibration standards by dilution from the stock solution of BA and TM in the relevant solvents. Samples were diluted when needed in order to bring them into the concentration range of calibration curves.

Before the above procedure, the amount of time required to reach maximum adsorption/equilibrium was optimized. This was done by weighing about 0.2 g of MCC in 20 falcon tubes. To each tube 10 mL of 1 g·L^{-1} of BA in MeCN was added. These tubes were vigorously shaken and then placed in a water bath at 25°C. Four of these samples were analyzed after each 30 min. Similar procedures were adopted for BA and TM in the other solvents and adsorbents.

3.2.3. Adsorption Study

Based on screening of the solvent, it was decided to determine the adsorption isotherm of BA in MeCN, EtOH, *n*-Hept using MCC as adsorbent. For Silica the adsorption isotherm of BA was only measured in *n*-Hept. For the determination of adsorption isotherm, an accurately known amount of approximately 0.1 g of adsorbent (MCC and Silica) were weighed individually into a 15 mL Falcon centrifuge tube. After that, 7 mL of the desired concentration of BA (0.01-0.75 g·L^{-1}) in the relevant solvent was added into the Falcon centrifuge tube using a glass pipette. The rest of the procedure is the same as described in section 3.2.2. The amount of BA adsorbed to the surface in each desired concentration was calculated using equation 2. For TM the adsorption isotherm was determined for both adsorbents only in *n*-Hept, in the concentration range 0.01-1.0 g·L^{-1}. The procedure is the same as described above and in section 3.2.2.

3.2.4. Desorption Study

For the desorption study, first 40 g of MCC was weighed and then 2 L of 1g·L^{-1} BA in *n*-Hept was added to it in a glass bottle. The solution was kept at 25°C in water bath for one hours and shaken at interval of 15 minutes to imitate the adsorption process. After one hour the solution was filtered through a 0.2 µm nylon membrane filter and the MCC containing adsorbed BA was collected and dried in oven at 60°C overnight. The amount of BA adsorbed to MCC was measured from the filtrate using UV-Vis spectrometer (UV-1800 Shimadzu) according to procedure presented above.

Two procedures were adopted for the desorption study. In the first procedure, 2 g of the above dried MCC powder was taken in a narrow long beaker. A rotor was installed in such a way that the rotating fan was about 2 cm above the surface of the powder. The rotating speed was fixed at 50 rpm and then 100 mL of the SBF was added to it. Two mL samples were taken from the beaker at different time intervals. These samples were then filtered through syringe filters and analyzed for amount of BA using UV-Vis spectrometer at 224 nm (UV-1800 Shimadzu). By this way the released rate of BA from the surface of MCC was determined in SBP.

In the second procedure, 1 gram of the above dried MCC was mixed with 19 g of latex in narrow long beaker to prepare model dispersion coatings. Mixing was done using a lab bench mixer at 1500 rpm for a period of 15 min and then dried at room temperature. The aim with latex binder was to manipulate the release of AM agent, where model coatings with binder should provide less exposed MCC particle and slower release rate of the AM agent, while MCC without latex is more exposed and hence would result in faster release of the AM agent.

For the desorption study with model dispersion coatings, the rotor was installed as above at 50 rpm. Then 100 mL of the SBP was added to each beaker and 2-3 mL samples were taken by pipette at different intervals. The samples were filtered and analyzed for amount of BA using spectrometer. By this way the effect of the amount of latex on the release rate of BA from MCC was measured. For the desorption process, all samples, solvent, model dispersion coating were stored at 4°C and the procedure was also carried out at 4°C so as to imitate the real storage conditions.

3.2.5. Calculations

All calculations were conducted using python version 3.10.9, using the libraries Matplotlib, Scipy, Numpy and Lmfit. Lmfit were used for all nonlinear regressions, Matplotlib for all plotting, and the AED were calculated using 10 000 iterations using the expectancy maximization method.

4. Results and Discussion

In this part, first we will present the adsorption capabilities of BA and TM on the two adsorbents in the given solvents.

Then we will show the adsorption isotherms of these solutes in the selected solvents on MMC and Silica. Finally, we will highlight the impact of latex binder on the release of BA from MCC in SBF.

4.1. Solvent Screening for Adsorption Process

The time required for adsorption process to reach equilibrium was investigated by measuring the adsorption of BA (1g·L^{-1} in MeCN) on MCC (about 0.2 g) at interval of 30, 60, 90, and 120 min, as described in section 3.2.2. The results are shown in figure 1. From figure 1 it is clear that although the equilibrium reached much earlier than 60 mins but we decided to use 60 min for further adsorption studies just to be more confident that equilibrium is always attained. Comparable results were observed for the other solvents and solute on both adsorbents.

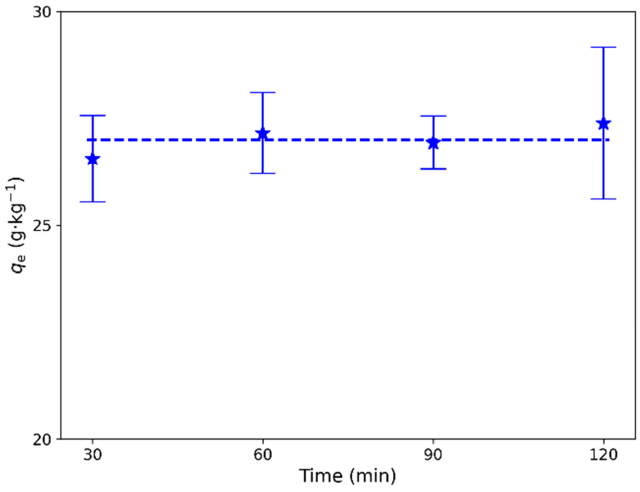

Figure 1. *Time to reach equilibrium for the adsorption studies. The error bars are 95% confidence interval. Experimental system: 10 mL of 1g·L^{-1} of BA in MeCN and 0.2 g MCC as adsorbent, the adsorbed amount are measured at different times.*

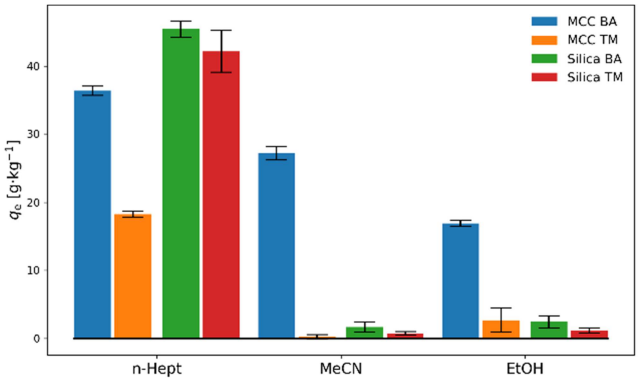

Figure 2. *Screening different solvents (n-Hept, MeCN and EtOH) for adsorption of BA and TM on MCC and silica. The error bars are 95% confidence interval. Experimental system: 10 mL solvent containing 1g·L^{-1} of BA or TM and 0.2 g adsorbent. Adsorption time 60 min.*

To determine the suitability of solvent for the adsorption process in terms of different polarities (i.e., polar protic solvent (EtOH), polar aprotic solvent (MeCN), non-polar solvent (*n*-Hept) and aqueous phosphate buffer at *p*H 7.5), their effect on the adsorption of BA and TM on MCC and Silica was investigated. The results of the adsorption, as described in section 3.2.2, are presented in figure 2.

As can be seen from figure 2, BA shows good adsorption on MCC in *n*-Hept, MeCN and EtOH as solvents. The trend is that adsorption decreases as the polarity of solvent increases where *n*-Hept has the highest adsorption and aqueous phosphate buffer has no adsorption. As compared to MCC, the adsorption of BA on silica is only high in non-polar *n*-Hept. TM on the other hand, shows good adsorption only in *n*-Hept on both MCC and silica. However, the adsorption of TM is much higher on silica than on MCC. No adsorption was recorded for both BA and TM on both adsorbents in aqueous phosphate buffer. Therefore, it was omitted from the graph and further adsorption studies. Based on these observations, we selected EtOH, MeCN and *n*-Hept for BA and only *n*-Hept for TM to further investigate the adsorption isotherms.

4.2. Adsorption Study

As discussed in the theory section an adsorption isotherm describes the relationship between the amount of solute adsorbed to the surface of the adsorbent and the concentrations of the solute in solution at equilibrium at given temperature. To get the full consensus of the adsorption isotherm one need to span the measurements from low to high concentration of the solute in the liquid phase.

Here, our approach involves analyzing the adsorption isotherm data through three steps: first, plotting the Scatchard plot to determine the type of adsorption model; second, calculating the AED to assess potential heterogeneity in the adsorption process; and finally, fitting the raw adsorption data to adsorption isotherm model that meets the criteria established earlier.

In figure 3, the adsorption isotherm analysis of TM in *n*-Hept on MCC is presented. In figure 3B, we can clearly see that the Scatchard plot is linear indicating that the Langmuir model could fit the adsorption data well.

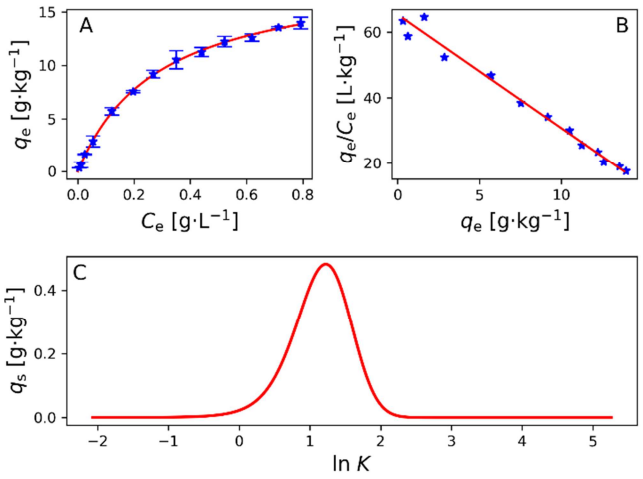

Figure 3. *Adsorption isotherm and analysis of adsorption isotherm for TM in n-Hept on MCC. A) raw adsorption isotherm data (symbols) with error bars (95% confidence interval) and solid lines model fitted to the Langmuir adsorption isotherm model. B) Scatchard plot, symbols experimental data solid line model fit to the Langmuir model. C) the calculated AED.*

To investigate this deeper the AED were calculated, see figure 3C. Here, we can clearly see that the AED is unimodal, indicating that Langmuir model is a good model choice. Fitting the raw adsorption data to the Langmuir model, see solid lines in figure 3A and 3B, the model fit the data well with an R^2 of 0.9993. Langmuir model were also found for TM in *n*-Hept on Silica, as well as BA in *n*-Hept on MCC, with R^2 values of 0.9982 and 0.9047, respectively.

In figure 4, the adsorption isotherm analysis of BA in MeCN on MCC is presented. In figure 4B, we can clearly see that the Scatchard plot is non-linear indicating that the Langmuir model could not fit the adsorption data well. To investigate this deeper the AED were calculated, see figure 4C. Here, we can clearly see that the AED is bimodal, so we need to use adsorption isotherms model with two different adsorption energies, such as the bi-Langmuir model. Fitting to the bi-Langmuir model, see solid lines in figure 4A and B, the model fit the data well. Also, the R^2 is 0.9649, indicating that the bi-Langmuir model describes the data well. Bi-Langmuir model was also found for BA in *n*-Hept on Silica, as well as BA in EtOH on MCC, with R^2 values of 0.9963 and 0.9765, respectively. Observe, that in these plots the low energy site of the AED calculation is not resolved. This is a rather common first adsorption because too low equilibrium concentration in the liquid phase were used in the adsorption isotherm acquisitions.

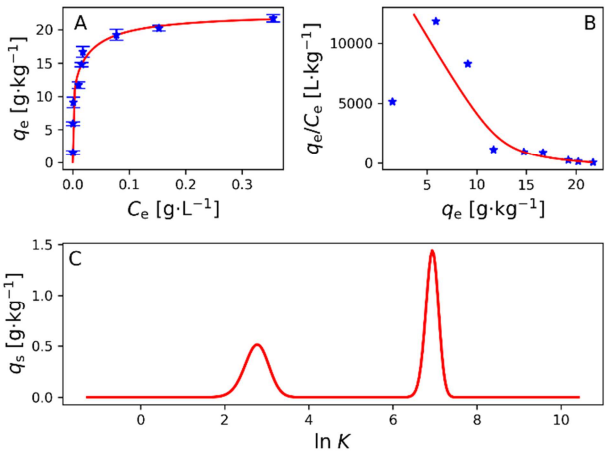

Figure 4. *Adsorption isotherm and analysis of adsorption isotherm for BA in MeCN on MCC. A) raw adsorption isotherm data (symbols) with error bars (95% confidence interval) and solid line model fitted to the bi-Langmuir adsorption isotherm model. B) Scatchard plot, symbols experimental data and solid line model fit to the bi-Langmuir model. C) the calculated AED.*

In figure 5, all adsorption isotherms for the adsorption of BA on MCC and Silica is presented. In figure 5, the general trend is the same as observed in solvent screening (section 4.1) where the adsorption capacity is higher in non-polar solvent and decreases with increasing polarity of solvent. The most likely reason may be the high and rapid solubility of BA in polar solvents (EtOH and MeCN) as opposed to non-polar *n*-Hept where the dissolution of BA requires sonication. On the other hand, the adsorption capacity of BA in *n*-Hept on silica is much higher than the adsorption of BA on MCC in *n*-Hept. The possible reason could be that silica has a surface area of more than 480 m^2g^{-1}, whereas MCC has a surface area of 53 m^2g^{-1}. This is almost 9 times greater than MCC. Also, the particle size of silica is much larger than MCC which may indicate higher porosity.

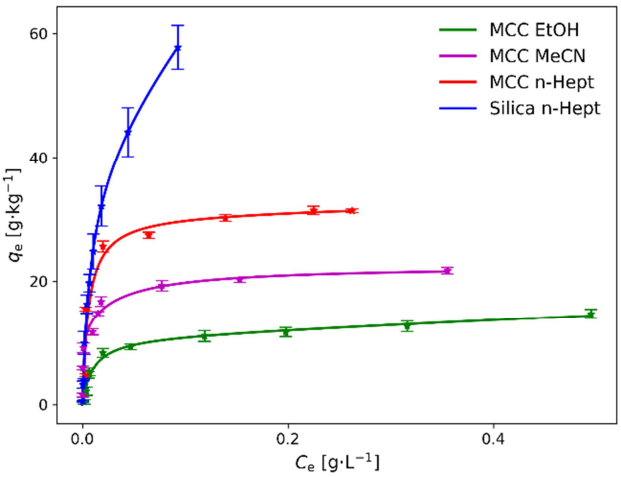

Figure 5. *Adsorption isotherm of BA on MCC and Silica. Solid lines represent the adsorption isotherm model fits, while symbols are experimental data with corresponding 95% confidence interval. Experimental system: 7 mL solvent containing different amount of BA and 0.1 g adsorbent. Adsorption time 60 min.*

The adsorption isotherm of TM on MCC and silica in *n*-Hept is shown in figure 6. TM has much higher adsorption capacity on silica than MCC in *n*-Hept, probably due to the much higher surface area of silica as compared to MCC.

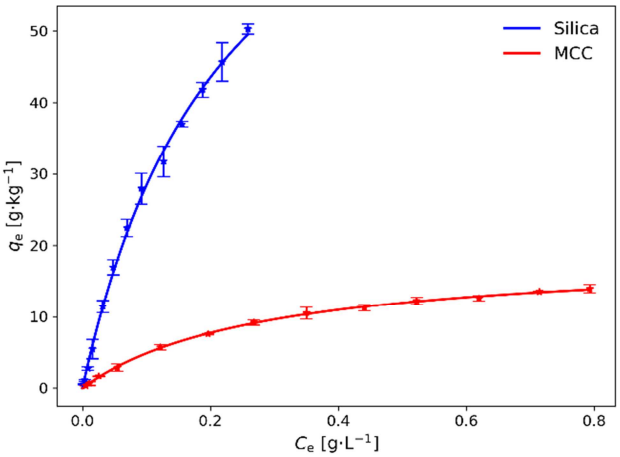

Figure 6. *Adsorption isotherm of TM on MCC and Silica are shown. Solid lines represent the adsorption isotherm model fits, while symbols represent the experimental data with their corresponding 95% confidence interval. Experimental system: 7 mL n-Hept containing different amount of TM and 0.1 g adsorbent. Adsorption time 60 min.*

In a previous study by Levy et al., the adsorption of aspirin and vanillin on FCC (similar to MCC) was investigated using chloroform (a polar aprotic solvent) and EtOH (a polar protic solvent) with varying water concentrations [30]. Instead of employing the detailed approach utilized in this study to determine the adsorption isotherm model, the authors directly applied the Tóth adsorption isotherm model to the data. The Tóth adsorption

isotherm model resulting in an unsymmetrical unimodal AED. The other major difference is that in this study also a nonpolar solvent *n*-Hept were used.

Comparing BA to aspirin and TM to vanillin, they share similar chemical traits, including polarity and essential functional groups. Levy et al. observed a decrease in vanillin's and aspirin's adsorption onto FCC with decreasing relative permittivity. If one ranks the solvents used in this study based on relative permittivity it is: MeCN (~37.5) > EtOH (~24.3) > *n*-Hept (~1.92). Our general findings (figure 2) show that the adsorption for TM follows this trend, with q_e values of 18.3 g·kg-1 in *n*-Hept, 1.7 g·kg^{-1} in EtOH, and 0.218 g·kg^{-1} in MeCN. However, for BA, this trend does not hold true, with q_e values of 36.4 g·kg^{-1} in *n*-Hept, 17.0 g·kg^{-1} in EtOH, and 27.2 g·kg^{-1} in MeCN. Therefore, the difference in relative permittivity cannot solely describe the trends in adsorption. other properties of solvents are also required to fully describe the trend.

4.3. Desorption Study

Antimicrobial packaging systems involve incorporating antimicrobial agents directly into packaging materials or in form of coatings where different binder can be used [31]. Here, we investigate the effect of adding latex binder on the release rate of BA from MCC (model dispersion coating) to assess its potential use in controlled release antimicrobial packaging. All the desorption procedures were carried out at 4°C which is the normal storage conditions of general fresh food items. figure 7 depicts the difference between the release of BA from MCC without and with latex.

The process is best described by first order desorption kinetics were the response %BA released could be expressed as:

$$\%\text{BA released} = 100(1 - e^{-k_d t}), \quad (5)$$

where k_d is the desorption rate constant, and t is the time.

The desorption data fit very well to a first-order desorption kinetic equation, see figure 7, resulting in R^2 values of 0.9798 and 0.9970 for desorption without and with latex, respectively.

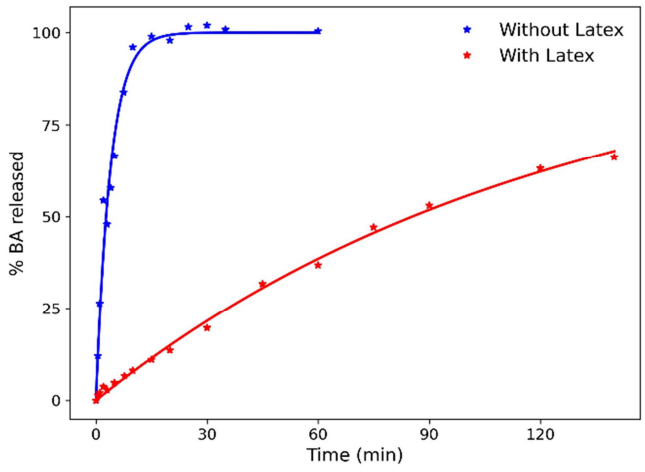

Figure 7. *Desorption of BA from MCC with and without latex binder at 4°C using SBF as desorbent liquid. Solid lines are model fit to the first order desorption kinetic equation and symbols are experimental data.*

The first-order kinetics assumes no re-adsorption to the adsorbent during the desorption process, a valid assumption in our system. This is substantiated by no adsorption of BA in water base buffer. Upon examining figure 5, it is also evident that the capacity of BA on MCC decreases with increase polarity of the solvent where EtOH (a polar solvent) has considerably lower monolayer saturation compared to *n*-Hept. Furthermore, the rapid release of BA without latex, fully completed within 10 minutes, further supports this assumption. The predicted k_d constants without and with latex were 0.253 min^{-1} (6.15% RSD) and 0.00811 min^{-1} (1.47% RSD), respectively. This indicates that the desorption rate for sample with latex was approximately 31 times slower than for that without latex. The slow release of antimicrobial agents from our model dispersion coating is indication of its potential use in the controlled release antimicrobial packaging.

5. Conclusions

A fundamental investigation of the adsorption of BA and TM on MCC and silica was carried out in solvents of different polarities. It was found that BA exhibits good adsorption on MCC in *n*-Hept, MeCN, and EtOH as solvents, while the adsorption of BA on silica was effective only in *n*-Hept. TM, on the other hand, demonstrates good adsorption solely in *n*-Hept on both MCC and silica. No adsorption was observed for either BA or TM on both adsorbents in the aqueous phosphate buffer. Based on these initial adsorption studies, the adsorption isotherms of BA were acquired using the batch method on MMC in *n*-Hept, MeCN, and EtOH, and only in *n*-Hept on Silica. For TM, the adsorption isotherm was acquired solely in *n*-Hept on both MCC and Silica. The adsorption data were modeled using Langmuir and bi-Langmuir isotherm models.

To investigate the desorption process, a model dispersion coating was prepared by mixing 1 part of MCC loaded with BA and 19 parts of latex binder. The desorption study indicates that BA is released 31 times slower from the model dispersion coating than from MCC without latex. This indicates the potential use of MCC as a carrier for antimicrobial agents in controlled release antimicrobial packaging.

Funding

This work was supported by the Swedish Knowledge Foundation via the project “MultiBarr” (grant number 20180036).

ORCID

ORCID 0009-0003-4863-5793 (Abdul Haseeb), 0000-0002-2432-390X (Beko Mesic), 0000-0003-1819-1709 (Jörgen Samuelsson)

Acknowledgments

We would like to acknowledge Fabian Monnar at Omya International AG Switzerland for fruitful discussions as well as Omya for providing MCC.

Conflicts of Interest

The authors declare no conflicts of interest.

References

[1] X. Sun, J. Wang, M. Dong, H. Zhang, L. Li, L. Wang, Food spoilage, bioactive food fresh-keeping films and functional edible coatings: Research status, existing problems and development trend, Trends in Food Science & Technology. 119 (2022) 122–132. https://doi.org/10.1016/j.tifs.2021.12.004.

[2] S. M. Abdel-Aziz, M. M. Asker, A. A. Keera, M. G. Mahmoud, Microbial food spoilage: control strategies for shelf-life extension, Microbes in Food and Health. (2016) 239–264.

[3] J. H. J. H. in't Veld, Microbial and biochemical spoilage of foods: an overview, International Journal of Food Microbiology. 33 (1996) 1–18. https://doi.org/10.1016/0168-1605(96)01139-7.

[4] S.-Y. Sung, L. T. Sin, T.-T. Tee, S.-T. Bee, A. R. Rahmat, W. Rahman, A.-C. Tan, M. Vikhraman, Antimicrobial agents for food packaging applications, Trends in Food Science & Technology. 33 (2013) 110–123.

[5] S. Quintavalla, L. Vicini, Antimicrobial food packaging in meat industry, Meat Science. 62 (2002) 373–380. https://doi.org/10.1016/S0309-1740(02)00121-3.

[6] A. KD, K. K. Jabo, Determination of Traditional and Biologically Viable Methods for Food Preservation: A Review, J Vet Heal Sci. 3 (2022) 384–389.

[7] G. L. Robertson, Food packaging and shelf life: a practical guide, CRC Press, 2009.

[8] C. N. Cutter, Microbial control by packaging: a review, Critical Reviews in Food Science and Nutrition. 42 (2002) 151–161.

[9] S. Naqash, F. Naqash, S. Fayaz, S. Khan, B. N. Dar, H. A. Makroo, Application of Natural Antimicrobial Agents in Different Food Packaging Systems and Their Role in Shelf-life Extension of Food: A Review, Journal of Packaging Technology and Research. 6 (2022) 73–89.

[10] R. Chawla, S. Sivakumar, H. Kaur, Antimicrobial edible films in food packaging: Current scenario and recent nanotechnological advancements- a review, Carbohydrate Polymer Technologies and Applications. 2 (2021) 100024. https://doi.org/10.1016/j.carpta.2020.100024.

[11] L. Kuai, F. Liu, B.-S. Chiou, R.J. Avena-Bustillos, T. H. McHugh, F. Zhong, Controlled release of antioxidants from active food packaging: A review, Food Hydrocolloids. 120 (2021) 106992. https://doi.org/10.1016/j.foodhyd.2021.106992.

[12] P. Widsten, B. B. Mesic, C. D. Cruz, G. C. Fletcher, M. A. Chycka, Inhibition of foodborne bacteria by antibacterial coatings printed onto food packaging films, Journal of Food Science and Technology. 54 (2017) 2379–2386.

[13] N. Rüegg, S. R. Teixeira, B. M. Beck, F. W. Monnard, R. Menard, S. Yildirim, Application of antimicrobial packaging based on modified calcium carbonate and EOs for RTE meat products, Food Packaging and Shelf Life. 34 (2022) 100982.

[14] J. H. Han, 4 - Antimicrobial food packaging, in: R. Ahvenainen (Ed.), Novel Food Packaging Techniques, Woodhead Publishing, 2003: pp. 50–70. https://doi.org/10.1533/9781855737020.1.50.

[15] S. Ahmed, D. E. Sameen, R. Lu, R. Li, J. Dai, W. Qin, Y. Liu, Research progress on antimicrobial materials for food packaging, Critical Reviews in Food Science and Nutrition. 62 (2022) 3088–3102.

[16] P. Suppakul, J. Miltz, K. Sonneveld, S. W. Bigger, Active packaging technologies with an emphasis on antimicrobial packaging and its applications, Journal of Food Science. 68 (2003) 408–420.

[17] R. D. Joerger, Antimicrobial films for food applications: a quantitative analysis of their effectiveness, Packaging Technology and Science: An International Journal. 20 (2007) 231–273.

[18] H. Brown, J. Williams, M. Kirwan, Packaged product quality and shelf life, Food and Beverage Packaging Technology. (2011) 59–83.

[19] P. a. C. Gane, C. J. Ridgway, E. Barceló, Analysis of pore structure enables improved tablet delivery systems, Powder Technology. 169 (2021) 77. https://www.academia.edu/16310239/Analysis_of_pore_structure_enables_improved_tablet_delivery_systems (accessed September 9, 2021).

[20] M. Fujiwara, K. Shiokawa, K. Morigaki, Y. Zhu, Y. Nakahara, Calcium carbonate microcapsules encapsulating biomacromolecules, Chemical Engineering Journal. 137 (2008) 14–22. https://doi.org/10.1016/j.cej.2007.09.010.

[21] Y. Ueno, H. Futagawa, Y. Takagi, A. Ueno, Y. Mizushima, Drug-incorporating calcium carbonate nanoparticles for a new delivery system, Journal of Controlled Release. 103 (2005) 93–98. https://doi.org/10.1016/j.jconrel.2004.11.015.

[22] B. Röcker, G. Mäder, F. W. Monnard, M. Jancikova, M. Welker, J. Schoelkopf, S. Yildirim, Evaluation of the potential of modified calcium carbonate as a carrier for unsaturated fatty acids in oxygen scavenging applications, Materials. 14 (2021) 5000.

[23] Y. Wang, A. Liu, R. Ye, X. Li, Y. Han, C. Liu, The production of gelatin-calcium carbonate composite films with different antioxidants, International Journal of Food Properties. 18 (2015) 2442–2456.

[24] G. Guiochon, A. Felinger, D. G. Shirazi, Fundamentals of preparative and nonlinear chromatography, Elsevier, 2006.

[25] T. Shibamoto, L. F. Bjeldanes, Chapter 9 - Food Additives, in: Introduction to Food Toxicology, Academic Press, 1993: p. Pages 157-182. https://doi.org/10.1016/B978-0-08-092577-6.50014-9. (https://www.sciencedirect.com/science/article/pii/B9780080925776500149).

[26] A. Heydari, J. Hadian, H. Esmaeili, M. R. Kanani, M. H. Mirjalili, A. Sarkhosh, Introduction of TMmus daenensis into cultivation: Analysis of agro-morphological, phytochemical and genetic diversity of cultivated clones, Industrial Crops and Products. 131 (2019) 14–24.

[27] A. Marchese, I. E. Orhan, M. Daglia, R. Barbieri, A. Di Lorenzo, S. F. Nabavi, O. Gortzi, M. Izadi, S. M. Nabavi, Antibacterial and antifungal activities of TM: A brief review of the literature, Food Chemistry. 210 (2016) 402–414.

[28] B. J. Stanley, G. Guiochon, Numerical estimation of adsorption energy distributions from adsorption isotherm data with the expectation-maximization method, The Journal of Physical Chemistry. 97 (1993) 8098–8104.

[29] T. Kokubo, H. Kushitani, S. Sakka, T. Kitsugi and T. Yamamuro, Solutions able to reproduce *in vivo* surface-structure changes in bioactive glass-ceramic A-W, *J. Biomed. Mater. Res.*, 24, 721-734 (1990).

[30] C. L. Levy, G. P. Matthews, G. M. Laudone, S. Beckett, A. Turner, J. Schoelkopf, P. A. C. Gane, Mechanism of adsorption of actives onto microporous functionalised calcium carbonate (FCC), Adsorption. 23 (2017) 603–612. https://doi.org/10.1007/s10450-017-9880-7.

[31] Tobi Fadiji, Mahdi Rashvand, Michael O. Daramola and Samuel A. Iwarere, A Review on Antimicrobial Packaging for Extending the Shelf Life of Food. In *Processes* 2023, 11, 590. https://doi.org/10.3390/pr11020590